Simulation of IR-heating and IR-scanning for the prediction of internal structures of walls

M. Penzel[1], F. Müller[1], M. Sui[1], M. Zinecker[1], A. Schubert[1], O. Wuttke[2], M. Gläser[3]
[1]Professorship Micromanufacturing Technology, Chemnitz University of Technology, 09107 Chemnitz, Germany
[2]Wuttke Ingenieure GmbH, Markt 5, 09111 Chemnitz, Germany
[3]IFU GmbH Privates Institut für Umweltanalysen, Gottfried-Schenker-Str. 18, 09244 Lichtenau, Germany

Abstract

A 3D-scanning of rooms and entire buildings is state of the art and commonly used to obtain and save the digital building structure [1–4].
With a new approach of IR-heating and IR-scanning the entire internal structure of walls, floors and ceilings could be captured and saved in a digital model. Plumbing, electrical work and refurbishing would become easier and safer. Searching and looking for old construction plans could become a part of the past. 3D-models could show the exact internal structure of the walls and help to save time and money when planning the enforcement of construction. To make this possible, a study is carried out to combine investigation of experiments of 3D-wall-scanning and the evaluation of simulation results to predict the possibilities and boundaries of the new scanning method. In this paper the setup of simulations, done in COMSOL Multiphysics, are discribed. For modelling radiation from wall to wall and the heat transfer inside the wall, the "heat transfer in solids" module is used. Radiation is applied perpendicular to the defuse wall surface with the boundary condition prescribed radiosity. This procedure is done with the help of a second wall that can be varied in distance. The prescribed radiosity is defined accordingly to the wave length of the radiator material and is varied as well. With the help of the models, it will be possible to make an assumption about the IR-source in terms of power, wavelength and required distance to the wall for IR-heating and IR-scanning in reality.

Introduction

Heat transfer is a subsection of thermodynamics and deals with the mechanisms that determine the magnitude of heat flow or heat transfer under given temperature differences and physical conditions. Heat transfer always takes place when a temperature difference prevails. It occurs both in a single system or between two systems which are in thermal contact. Heat transfer can basically take place by conduction, convection and radiation, usually it is a combination of several mechanisms. In convection, the heat exchange takes place both by heat conduction and by the fluid flow. In heat conduction in solids or static fluids, the heat transfer depends only on the material properties and the temperature gradient. Heat transfer between a solid and a flowing fluid takes place by conduction between the solid and fluid. A distinction is made between free and forced convection. In free convection, the fluid flow is due to a difference in temperature and density. In forced convection, the flow is created by external pressure difference. Radiation takes place without material carrier, by electromagnetic waves between surfaces. [5–7] Heat transfer between walls and fluids, e.g. in flushed water pipes or heating pipes, but also to the environment, takes place when there is a temperature difference in the building structures. Thermal contact resistances from solid to solid, but also from solid to fluid, determine the heat transfer. Furthermore, the heat transfer depends on material characteristics. These include, for example, the thermal conductivity or the heat capacity. Material-dependent characteristic values are again temperature- and time-dependent. Also external boundary conditions, such as the humidity and ambient temperature are important. Even geometric boundary conditions, such as size or thickness of the wall are essential.
Another relevant phenomenon in this investigation is the absorption of heat radiation in bodies. Radiation that strikes a surface is reflected to a certain extent depending on the surface and material properties. Part of the radiation is transmitted through the body and the rest is absorbed. [6] When the radiated body absorbs the light, the energy of the light is absorbed by the molecules of the body and converted into kinetic energy. The activated molecules thereby generate heat that is released from the body to the environment. The different radiation sources can be divided according to the wavelength or the frequency. [8]
In this study 3D time dependent modelling of walls, containing entire infrastructure for water supply and electricity, was carried out. The results of the simulations have been analysed and evaluated.

Geometry and material

Several model geometries for IR-heating and IR-scanning were created in COMSOL Multiphysics. The representation of a selected model geometry is given in Figure 1.

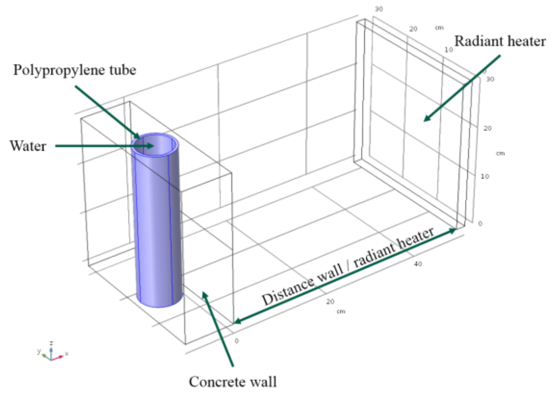

Figure 1: Presentation of a selected model geometry with different boundary and domain conditions

The dimensions of the concrete wall with the tube inside are 30 cm in length, 30 cm in height and the thickness is 10 cm. The outer diameter of the polypropylene tube is 8 cm with a wall thickness of 0.5 cm. The thickness of the radiant heater is 2 cm, but can be neglected since only the plane facing towards the concrete wall has a function in the simulation. The distance between the concrete wall and the radiant heater is varied in different studies from 50 cm up to 150 cm. In Figure 1 the distance of 50 cm is given. The domain inside the tube is defined to be water. In the distance between the concrete wall and the radiant heater no material is required, since radiation will be used for the heat transfer. The thermal properties of the used materials are summarised in Table 1 [9].

Table 1: Materials and thermal properties

Material	Thermal conductivity [W/(m·K)]	Heat capacity [J/(kg·K)]
Concrete	1.8	880
Polypropylene	0.13	1574
Water (20 °C)	0.55	4187

In the simulation the thermal properties are kept constant.

Physic, domain and boundary conditions

Heat transfer in solids is used as the basic physic in the simulation to investigate the thermal behaviour of the concrete wall and the internal structure during the time dependant heating process. Additional, the water domain is defined as fluid. The definitions of the different domains are shown in Figure 2.
Sub-definitions are made to the solid materials to be non-transparent on all three spectral bands and to the fluid to be transparent on all three spectral bands as well.

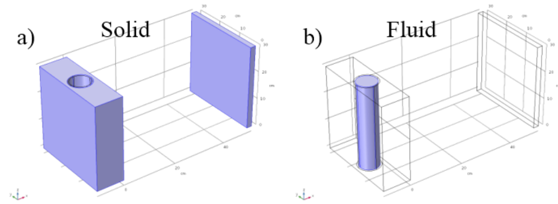

Figure 2: Domain definitions

This enables to define surface-to-surface radiation in the model.
The next figure shows the different boundaries selected for different boundary conditions.

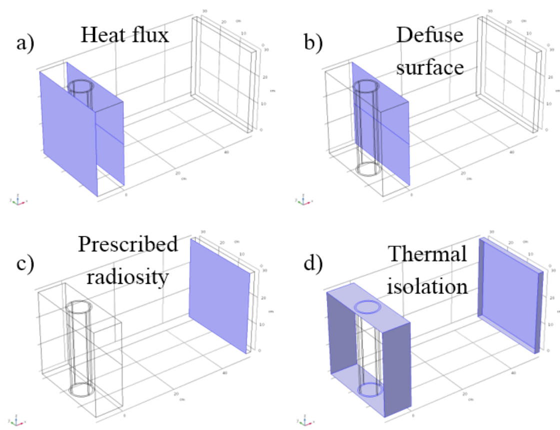

Figure 3: Boundary conditions

The heat flux is defined as convective heat flux with external convection at a vertical wall. The height of the wall is set to 30 cm.
In Figure 3 b) the surface of the concrete wall is defined to be a defuse surface.

All three bands of surface absorption can be defined separately. Values for the surface absorption of concrete are given in Table 2.

Table 2: Proportion of surface absorption for concrete at different wavelength

Proportion of wavelength	[%]
Absorption A (< 2 µm)	66.5
Absorption B (2 µm to 4 µm)	84.8
Absorption C (> 4 µm)	92.1

The reflectance ρ_r of the concrete decreases with increasing wavelength. The emissivity ε equal to the absorption I is calculated from the following equation when the transmittance is zero.

$$I = 1 - \rho_r \quad (1)$$

Special values for the reflectance ρ_r of concrete can be found in the Ecostress Spectral Library. [10]

The prescribed radiosity is defined separately for all three spectral bands according to the infrared proportion and the power density of the radiant heater. In the given example this will be the parameters for a metal/ceramic radiator, sine ceramic radiators have highest values in infrared C. Parameters for the different wavelengths are given in Table 3.

Table 3: Proportions of infrared radiation for meatal/ceramic radiator

Proportion of wavelength	[%]
Infrared A (< 2 µm)	2.2
Infrared B (2 µm - 4 µm)	37.2
Infrared C (> 4 µm)	60.6

The power density is defined to vary from 1000 W/m² to 2000 W/m². A schematic representation of the radiation spreading is given in Figure 4.

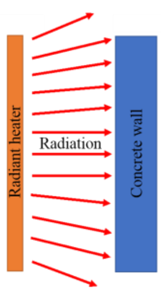

Figure 4: Schematic representation of radiation from the radiant heater to the wall

For the same power density but different distances from the radiant heater to the concrete wall, the density of radiation is varying at the surface of the wall.
The last boundary condition for the model is thermal isolation. Surfaces of this boundary condition are shown in Figure 3 d).

Mesh

The basic definition of a mesh COMSOL Multiphysics is triangular mesh elements. This option results in an inhomogeneous net displacement at the surface of the concrete wall and must be avoided. This is done by structuring the surface of the concrete wall in quad elements. A detailed view of the meshed model is given in Figure 5.
At the left side basic information about the mesh can be found. The total number of domain elements is 27380.

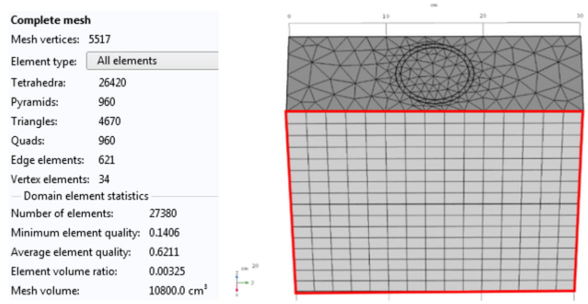

Figure 5: Illustration of mesh structure in numbers and as 3D plot

The surface of the radiant heater is structured with quad elements as well to guarantee homogeneous radiant distribution.

Results

To analyse the temperature distribution inside the concrete wall, one line and two planes for temperature evaluation are defined as shown in Figure 6.

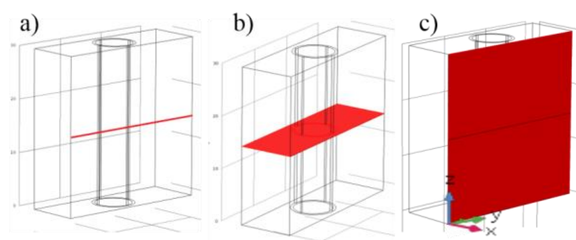

Figure 6: Line and planes for temperature evaluation

For all the models heating time of 2000 s is simulated, starting at 0 s with a step size of 100 s. The results for the power density of 2000 W/m² and a wall radiator distance of 50 cm are shown in Figure 7.

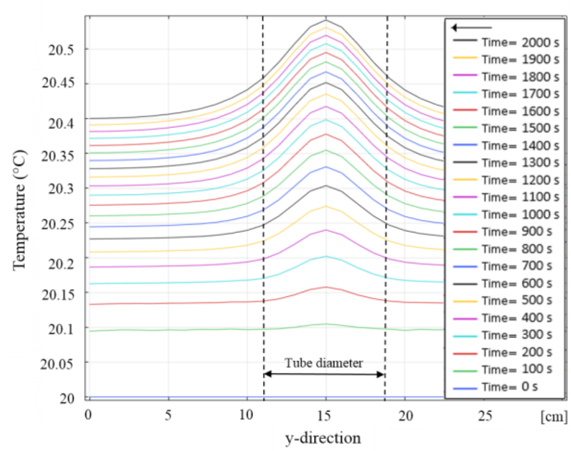

Figure 7: Temperature distribution along the evaluation line

Figure 7 shows that the temperature difference along the measurement line on the surface of the concrete wall increases with prolonged radiation time and the concrete surface is heated. In the area of the polypropylene tube, a significant temperature maximum is observed in the graph. This is due to the fact that the thermal conductivity of polypropylene is less than 10 % in comparison to concrete. The tube acts a thermal barrier and heat accumulates in front of the tube. The longer the thermal energy is applied to the surface of the wall, the more noticeable the effect will be. It also can be found that the wall temperature will approach a maximum since the temperature difference is getting closer between every time step.
The temperature distribution inside the wall is shown in Figure 8 as a cross cut for four selected times.

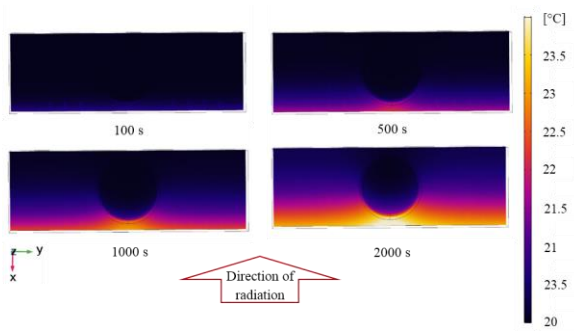

Figure 8: Cross cut views at different times of radiation

It can be seen that with increasing radiation time the maximum temperature difference in the cross cut plane increases. In detail, it can be found that with increasing radiation time the concrete is also increasing the temperature into the component depth. The polypropylene tube acts in this material combination as a thermal insulator and leads to a heat accumulation in the near wall region in front of the pipe. This thermal behaviour coincides with the results of the temperature evaluation from Figure 6.
The results of varying the distance between the concrete wall and the radiant heater at fixed power density of 1000 W/m² and after 2000 s are shown in Figure 9.

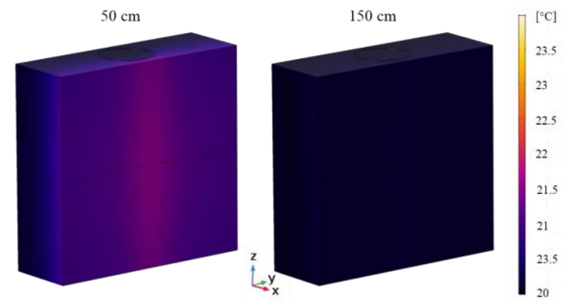

Figure 9: Temperature distribution in the concrete wall for a power density of 1000 W/m², a radiation time of 2000 s and distances of the heat radiator to the wall of 50 cm (left) and 150 cm (right)

From the results of the simulations, it can be deduced that the selected power density of 1000 W/m², regardless of the selected distance between concrete wall and radiant heater, is insufficient to generate a significant increase in temperature and temperature difference on the concrete wall surface. In a next step, it is checked whether an increase in the power density up to 2000 W/m² would have a positive influence on the temperature differences. The results are shown in Figure 10.

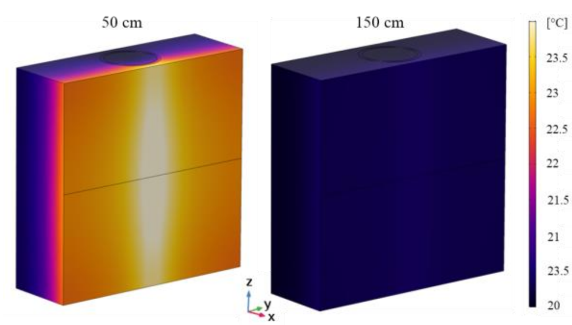

Figure 10: Temperature distribution in the concrete wall for a power density of 2000 W/m², a radiation time of 2000 s and distances of the heat radiator to the wall of 50 cm (left) and 150 cm (right)

From the comparison of the simulation results, it can be seen that the chosen power density of the radiant heater of 2000 W/m² and a distance of the radiant heater to the wall of 50 cm cause the highest temperature difference.
Figure 11 compares the power density depending on the radiation distance.

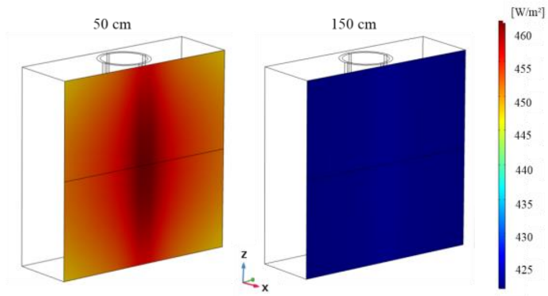

Figure 11: Radiation distribution on the concrete wall for a power density of 2000 W/m², a radiation time of 2000 s and distances of the heat radiator to the wall of 50 cm (left) and 150 cm (right)

From Figure 11 it can be seen that the radiation intensity is not distributed homogeneously on the surfaces of the concrete walls for the both distances. The achieved power densities on the surface with a distance of 150 cm to the radiation source is about 40 W/m² less, but the distribution of the power density is more homogeneous. As the distance increases, the power density of the radiator must also increase in order to generate a measurable power input at the concrete surface.

Conclusions

The results of the simulations show that the power density of the radiant heater, the distance of the radiant heater to the concrete wall and the radiation time are of great importance.
From the results it can be seen, that a power density of 1000 W/m² is insufficient to generate a significant temperature increase or temperature difference on the surfaces of the concrete walls.
Shorter distances achieve higher power input to the wall. In a practical application this would also be unsuitable since the radiant heater must first be moved aside before thermal measurements can be done and the radiation would not be distributed homogeneous at the surface of the concrete wall.
A compromise of sufficiently large distance combined with a correspondingly high power density of the radiator is therefore desirable.

Future simulations will consider different internal structures and materials in the concrete and brick walls to gain more knowledge about the possibilities of thermal 3D-scanning of building structures. Further the comparison of thermal measurements from real walls and results of simulations will be done to find a practicable setup for IR-heating and IR-scanning of walls.

Acknowledgement

The presented contents are results of a research project funded by the Federal Ministry of Economic Affairs and Energy, following a decision of the German Bundestag.

References

[1] P. Battalwar, J. Gokhale, and U. Bansod, ‘Infrared Thermography and IR Camera’, *Int. J. Res. Sci. Eng.*, vol. 1, no. 3, pp. 9–14, 2015

[2] K. Kurita, M. Oyado, H. Tanaka, and S. Tottori, ‘Active infrared thermographic inspection technique for elevated concrete structures using remote heating system’, *Infrared Phys. Technol.*, vol. 52, no. 5, pp. 208–213, 2009, ISBN: 13504495, ISSN: 13504495, DOI:10.1016/j.infrared.2009.07.010

[3] F. Ciampa, P. Mahmoodi, F. Pinto, and M. Meo, ‘Recent advances in active infrared thermography for non-destructive testing of aerospace components’, *Sensors (Switzerland)*, vol. 18, no. 2, 2018, ISSN: 14248220, DOI:10.3390/s18020609

[4] M. . Hain, J. . Bartl, and V. Jacko, ‘Active Infrared Thermography in Non-destructive Testing’, *Meas. 2009, Proc. 7th Int. Conf.*, pp. 339–343, 2009

[5] P. von Böckh, *Wärmeübertragung Grundlagen und Praxis*, 5. Auflage. Berlin, Heidelberg, 2009, ISBN: 9783642030437

[6] E. Völker, ‘Numerische Berechnungen der Temperaturverteilung in einem Wasserbehälter mit transparenter Abdeckung bei direkter Sonnenstrahlung’, Brandenburgische Technische Universität; Moskauer Energetisches Universität, 2013

[7] H. Oertel, *Prandtl - Führer durch die Strömungslehre - Grundlagen und Phänomene*, 14th ed. Springer Vieweg, 2017, ISBN: 978-3-658-08626-8, DOI: 10.1007/978-3-658-08627-5

[8] N.N., ‘Einteilung elektromagnetischer Strahlung nach Wellenlänge’. [Online]. Available:

https://de.wikipedia.org/wiki/Elektromagnetische_Welle. [Accessed: 22-Feb-2019]
[9] VDI, *VDI-Wärmeatlas*, 11th ed. Berlin Heidelberg: Springer Vieweg, 2013, ISBN: 9783642199806
[10] N.N, ‘Spectral Results’. [Online]. Available: https://speclib.jpl.nasa.gov/library/ecoviewplot. [Accessed: 13-Dec-2018]